RC24849 (W0908-129) August 25, 2009
Materials Science

IBM Research Report

Interfacial Reactions and Microstructures of Sn-0.7Cu-xZn Solders with Ni-P UBM during Thermal Aging

Moon Gi Cho[1], Sung K. Kang[2], Sun-Kyoung Seo[1], Da-Yuan Shih[2], Hyuck Mo Lee[1]

[1]Department of Materials Science and Engineering
KAIST
335 Gwahangno, Yuseong-gu
Daejeon
Republic of Korea 305-701

[2]IBM Research Division
Thomas J. Watson Research Center
P.O. Box 218
Yorktown Heights, NY 10598
USA

Research Division
Almaden - Austin - Beijing - Cambridge - Haifa - India - T. J. Watson - Tokyo - Zurich

Interfacial Reactions and Microstructures of Sn-0.7Cu-xZn Solders with Ni-P UBM during Thermal Aging

Moon Gi Cho, Sung K. Kang*, Sun-Kyoung Seo, Da-Yuan Shih* and Hyuck Mo Lee

Department of Materials Science and Engineering, KAIST

335 Gwahangno, Yuseong-gu,

Daejeon, Republic of Korea 305-701

*IBM T.J. Watson Research Center

1101 Kitchawan Road, Route 134,

Yorktown Heights, NY 10598, USA

Corresponding Author: Prof. Hyuck Mo Lee

E-mail: hmlee@kaist.ac.kr

Tel: +82-42-350-3334

Fax: +82-42-350-3310

Abstract

The effects of Zn addition to Sn-0.7Cu are investigated, focusing on their interfacial reactions, microstructure and mechanical properties, when reacted with Ni-P under bump

metallurgies (UBMs). The Zn content in Sn-0.7Cu-xZn varies as 0.2, 0.4 and 0.8 (in wt %). In the reaction with Ni-P UBMs, $(Cu,Ni)_6Sn_5$ intermetallic compounds (IMCs) are formed at the interface of the Sn-0.7Cu solder, while $(Cu,Ni,Zn)_6Sn_5$ IMCs in the Zn-doped solders. As the Zn content increases, the interfacial IMC growth is gradually reduced, yielding a reduction of 40-50% for 0.8% Zn. The same IMC particles are also observed in the matrix of each solder. In Sn-0.7Cu, $(Cu,Ni)_6Sn_5$ particles coarsen largely during aging, while $(Cu,Ni,Zn)_6Sn_5$ particles in the Zn-added solders are less coarsened and remain much smaller than $(Cu,Ni)_6Sn_5$. The growth of $(Cu,Ni)_6Sn_5$ during thermal aging is significantly suppressed by Zn addition. In addition, such a microstructure in the Zn-doped solders with Ni-P produces the stable mechanical properties, such as hardness and shear strength, during thermal aging.

Keywords: Pb-free solders, Zinc, electroless Ni-P, interfacial reactions, microstructure

1. Introduction

The RoHS legislation passed by EU in 2002 has come into effect to ban the use of Pb and other toxic materials in electronic packaging. The extensive searches for Pb-free solder

candidates have been conducted in last several years.[1-4] However, aggressive interfacial reactions in Sn-rich solder joints, such as the formation of large intermetallic compounds (IMCs),[5,6] rapid consumption of UBMs, and void formation at the interface,[5,6] have been recognized as critical factors afftecting the reliability of Pb-free solder joints. Recently, many studies have been conducted to solve these problems by adding minor alloying elements (less than 1 wt%) to Pb-free solders alloys, such as Ni,[7] Ti,[7] Mn,[7] Co,[7,8] Zn,[8-11] Fe,[8] and In-Ni.[8] Among the various minor alloying elements, the minor Zn addition is found to be most effective on controlling the interfacial reactions with Cu UBMs. Actually, the formation of Cu_3Sn IMCs, the consumption of Cu UBM and the interfacial void formation are reduced by adding a small amount of Zn.[8-11]

Because of its slow reaction rate with Sn-rich solders, Ni UBMs (electroplated or electroless) are commonly used in Pb-free solder joints. However, the effects of minor Zn addition (less than 1 wt%) on the interfacial reactions with electroless Ni-P UBMs have not been systematically studied. In the literature, there are only a few studies reported on the Zn addition in Sn-rich solders with Ni-P UBM. Song et al. compared the effect of a minor addition of Co, Ni and Zn on interfacial reactions in Sn-3.0Ag-0.5Cu and Ni-P, but more interested in Co or Ni, not much on Zn.[12] Kang et al. have reported the effects of a minor addition of Zn on the interfacial reactions of Sn-3.8Ag-0.7Cu with Cu vs. Ni-P, but focused much more on the interfacial reactions with Cu UBMs.[10]

In this study, the effects of minor Zn addition on the interfacial reaction of Sn-0.7Cu with electroless Ni-P UBMs during thermal aging at 150°C are investigated. Especially, the microstructure changes of Zn-doped solders reacted with Ni-P UBMs are analyzed by EPMA and TEM, and are explained by thermodynamic calculations. In addition, the

mechanical properties (hardness and shear strength) of Zn-doped vs. un-doped solders are compared as a function of aging time.

2. Experimental Procedures

The solder compositions used in this study are Sn-0.7Cu, Sn-0.7Cu-0.2Zn, Sn-0.7Cu-0.4Zn and Sn-0.7Cu-0.8Zn (in wt %)., Solder balls were commercially produced with the size of 380 μm in diameter. The substrate was also commercially fabricated as a printed circuit board (PCB) having bond pads of 300 μm in diameter. The Cu pad (20 μm) has the surface finish of Ni-P (5 μm)/Au (0.05 μm). This bond pad serves as under bump metallization (UBM) of the solder joint. The solder balls were reflowed on the pads in a reflow machine. The reflow profile parameters used are 1.5 min dwell time (above m.p. ???), a peak temperature of 250°C and a cooling rate of 1°C/s. Subsequently, an aging experiment was conducted in a nitrogen oven at 150°C for up to 1000 h.

After reflow and aging, the microstructure of solders as well as the interface with Ni-P UBMs were examined on their cross sections metallographically prepared by mounting and polishing. Optical microscopy (OM), scanning electron microscopy (SEM) and transmision electron microscopy (TEM) were employed to characterize the IMCs. The back-scattered electron mode of SEM was used to observe the IMCs, and energy-dispersive X-ray spectroscopy (EDS) and electron probe micro-analyzer (EPMA) for compositional analyses.

Microhardness tests were performed to compare Vickers hardness numbers (VHNs) of the samples aged at 150°C for up to 1000 h. The load of hardness tests was 10 g with a loading time of 5 s. Figure 1(a) shows the location of indentations in a solder joint. The VHN was

reported as an average value of eighteen indentations or more. For joint shear tests, DAGE 4000 series shear tester was used. Figure 1(b) is a schematic diagram showing the arrangement of the shear test. Test conditions were a maximum load of 5 kg, shear height of 20 μm, and stylus speed of 200 μm/s.

3. Results and Discussion

1) IMCs formation and growth during Thermal Aging at 150°C

Figure 2 is the collection of typical cross-section images of four different solders reacted with electroless Ni-P UBMs after the reflow and aging. The first row exhibits the SEM images of the interface between four solders (Sn-0.7Cu, SC; Sn-0.7Cu-0.2Zn, SC-0.2Zn; Sn-0.7Cu-0.4Zn, SC-0.4Zn; and Sn-0.7Cu-0.8Zn, SC-0.8Zn) and Ni-P UBMs after the reflow. The second and third rows exhibit the SEM images after aging at 150°C for 500 h and 1000 h, respectively.

For the as-reflowed, thin IMCs were observed commonly at the interface of all solders. The IMCs formed at the interfaces of Sn-0.7Cu and SC-0.2Zn have a thin rod shape, whereas, in SC-0.4Zn and SC-0.8Zn, they appear as a thin layer. When the aging was conducted up to 1000 hours, the IMCs in all solders became thicker than in the as-reflowed. In addition, the shape of all IMCs changed to a layer type, yielding no difference in the shape of the interfacial IMCs formed with a different Zn content.

To identify the IMC phases formed at the interface, the compositional analysis was conducted by EPMA(Is this EPMA or EDS ??????? In Table caption, it is written as EDS). The Sn-0.7Cu-xZn solders with Ni-P UBMs aged for 1000 h were employed and the results were summarized in Table 1. A, B, C, and D mean the locations marked in Fig. 2. Each number

reported in Table 1 is an average of five measurements from each location. The IMCs formed at the interface between the Sn-0.7Cu solders and Ni-P UBMs were identified as the ternary Sn-Cu-Ni compounds, consisting of Sn (45.8 at%), Cu (42.7 at%) and Ni (11.4 at%). The ternary IMCs appear to be $(Cu,Ni)_6Sn_5$ in the view of their atomic ratios. It has been reported that when Sn-rich solders with Cu of more than 0.4 wt%, the $(Cu,Ni)_6Sn_5$ IMC was formed at the interface even though solders were reacted with Ni-based UBMs during reflow.[13,14] In this study, considering the Cu content (0.7 wt.%), the measured atomic ratios and their morphology of Sn-Cu-Ni IMCs, the ternary compounds are believed to be a $(Cu,Ni)_6Sn_5$.type, not a Ni3Sn4 type. However, in the Zn-doped solders, Zn atoms were detected in the IMC phases formed at the interface. The EPMA compositional analysis shown in Table 1 indicates that the IMCs formed at the interface between the Zn-doped solders and Ni-P UBMs are quarternary Sn-Cu-Ni-Zn compounds, with an increasing Zn content when the Zn % in the solders increase. Since the atomic ratios of the quaternary IMCs are very similar to Cu_6Sn_5 or $(Cu,Ni)_6Sn_5$, the quaternary IMCs is regarded to be $(Cu,Ni,Zn)_6Sn_5$.

In terms of IMCs growth, a little difference was observed as a function of Zn content in the solders. To compare the IMCs thickness of each solder quantitatively, the thickness of IMCs was measured by an image analysis software program, and summarized in Fig. 3. The IMCs thickness decreased gradually with an increase of the Zn content in the Sn-0.7Cu-xZn solders. In other words, IMCs growth during thermal aging was reduced by the Zn addition to Sn-0.7Cu. As discussed earlier, $(Cu,Ni,Zn)_6Sn_5$ IMCs, instead of $(Cu,Ni)_6Sn_5$, were formed at the interfaces of Zn-doped solders reacted with Ni-P UBMs. The incorporation of Zn into $(Cu,Ni)_6Sn_5$ IMCs would be attributed to a slight reduction of IMC growth during aging. However, the amount of reduction in the IMCs growth owing to the addition of 0.2 or 0.4 wt% Zn was not significant (less than 30 %). For 0.8Zn addition, about 50% reduction of

IMC growth was observed in case of 1000 h aging. Since the maximum IMCs thickness observed in Sn-0.7Cu solders with Ni-P was only less than 2.5 μm after thermal aging for 1000 h, the Zn addition would not be so effective on further reducing the IMCs growth in the interfacial reactions of Sn-0.7Cu on Ni-P UBMs during thermal aging.

2) Microstructures of Sn-0.7Cu-xZn Reacted with Ni-P UBMs

Figure 4 is the typical OM images of four solders far inside from the interface; as-reflowed (top) and aged at 150°C, 500 h (bottom). For the Sn-0.7Cu as-reflowed, a unique microstructure was observed, consisting of β-Sn dendrites (light contrast) and eutectic phases (dark contrast, a mixture of the intermetallic particles). After the thermal aging, the microstructures of the Sn-0.7Cu solders have significantly changed.. The β-Sn dendrite cells disappeared, and many large IMC particles were observed in Sn matrix. In addition, the IMC particles notably coarsened compared to those of the as-reflowed.

In case of Zn-doped solders reacted with Ni UBMs, the as-reflowed microstructures were very similar to the Sn-0.7Cu, consisting of β-Sn dendrites (light contrast) and eutectic phases (dark contrast). However, β-Sn dendrites and the eutectic region in Zn-doped solders were larger than those of the un-doped Sn-0.7Cu. Two explanations are possible for these changes in Zn-doped solders. The first explanation is related to the amount of alloying elements in solder. In general, the volume fraction of the eutectic phase increases as the alloying elements in solder increase. Therefore, the addition of Zn to Sn-0.7Cu solders can increase the volume fraction of the eutectic phase. The second explanation is related to the amount of undercooling during solidification. It has been reported that a small addition of Zn into Sn-rich solders is very effective to reduce the undercooling of the solders.[8,9] By adding the small

amount of 0.1 wt% Zn into Sn-3.0Ag-0.5Cu solders, the undercooling was significantly reduced to less than 3°C.[8] In this way, the undercooling of the Zn-doped solders must be much smaller than that of Sn-0.7Cu. Furthermore, the nucleation and growth of solidifying phases in the Zn-doped solders occur at a higher temperature than the actual freezing temperature of Sn-0.7Cu solders. In general, the growth of solidifying grains becomes faster at a higher temperature, and then a large grain structure can be formed. Consequently, a solder alloy solidified with a smaller undercooling has a coarser microstructure than with a larger undercooling. Actually, Xiao et al.[15] and Cho et al.[16] reported that the solders with a smaller amount of undercooling exhibited the coarser microstructures of large β-Sn dendrites and a thick network of the eutectic phases. In fact, the increase in the Zn content in our study does not affect the size of β-Sn dendrites, but the volume fraction of the eutectic phase. Therefore, the reduction of undercooling by the Zn addition appears to be a dominant factor over the total Zn content in determiing the microstructure of the Zn-doped solders..

Afther the thermal aging, another interesting difference was observed between the Zn-doped and the un-doped solders. In the aged Sn-0.7Cu with Ni-P, β-Sn dendrites disappeared and the dispersed IMC particles significantly coarsened in the solder matrix. Meanwhile, in case of the Zn-doped solders, the microstructural changes were less pronounced as Zn content increases. In the aged SC-0.2Zn , the β-Sn dendrites mostly disappeared, but IMC particles in the solder matrix somewhat coarsened (marked by the arrow in Fig. 4). In the SC-0.4Zn aged with Ni-P, more β-Sn dendrites remained and coarsening of IMC particles was suppressed much more. Namely, most of IMC particles in the solder matrix were much smaller than those in the aged Sn-0.7Cu. Interestingly, in the aged SC-0.8Zn, the β-Sn dendrites hardly disappeared, and, moreover, the IMC particles were as small as those of the as-reflowed. The

microstructure of the aged SC-0.8Zn was very similar to the as-reflowed. In other words, the 0.7 wt % Zn addition into Sn-0.7Cu was effective to reduce coarsening of IMCs particles and to stabilize the microstructure during the thermal aging.

To further understand the effect of Zn addition on the microstructural changes during thermal aging, the IMC phases formed inside the Zn-doped solders were estimated by the thermodynamic calculations. The thermodynamic calculations were conducted by the Thermo-Calc thermodynamic software developed at the Royal Institute of Technology, Stockholm, Sweden.[17] Figure 5(a) is the equilibrium phase diagram of a Sn-Cu binary system and Fig. 5(b) is the vertical section of the Sn-Cu-Zn ternary phase diagram calculated along a constant ratio of 99.3 Sn :0.7 Cu. As shown in Fig. 5, the equilibrium phases of Sn-0.7Cu solder at 150°C are β-Sn and Cu_6Sn_5, and for SC-0.4Zn are β-Sn, Cu_5Zn_8 and Cu_6Sn_5. By adding the small amount of Zn into Sn-0.7Cu, a new IMC phase, Cu_5Zn_8, forms in Zn-doped solders, in addition to Cu_6Sn_5 IMCs formed in both solders.

However, the microstructures of Sn-0.7Cu and Zn-doped solders were much different from the calculated equilibrium microstructures after thermal aging at 150°C. Thus, further investigations, such as EPMA and TEM, were conducted to find out the reason. The chemical composition of IMC phases formed in the solder matrix after thermal aging at 150°C for 1000 h was analyzed by EPMA. Figures 6 and 7 are the EPMA mapping images of Sn-0.7Cu and SC-0.4Zn solders far inside from the interface, respectively. Similarly with the previous OM images, large IMC particles are observed in the Sn-0.7Cu reacted with Ni-P, while small IMC particles in the SC-0.4Zn. In addition, the large IMC particles in the aged Sn-0.7Cu are consisted of Cu, Ni and Sn, whereas the small IMC particles in the aged SC-0.4Zn consisted of Cu, Ni, Zn and Sn. By the compositional analysis of EPMA, the large IMC particles were

identified as the ternary Sn-Cu-Ni compounds of Sn (46.5 at%), Cu (46.0 at%) and Ni (7.5 at%). Meanwhile, the small IMC particles were identified as the quaternary Sn-Cu-Ni-Zn compounds of Sn (44.4 at%), Cu (46.0 at%), Ni (3.9 at%) and Zn (5.7 at%). In the atomic ratio, the Sn-Cu-Ni ternary compounds and Sn-Cu-Ni-Zn quaternary compounds would be $(Cu,Ni)_6Sn_5$ and $(Cu,Ni,Zn)_6Sn_5$, respectively.

To clearly identify the IMCs formed in the aged Sn-0.7Cu and SC-0.4Zn, both IMC phases were further investigated by TEM. The specimens used for TEM were prepared by focused ion beam (FIB) method, and IMC particles of the dotted circles in Figs. 6 and 7 were selected. Both IMC particles were characterized with TEM operated at 200 kV. Figure 8 shows the TEM micrographs and electron diffraction patterns of the IMC particles formed in the aged Sn-0.7Cu and SC-0.4Zn solders, respectively. By an EDS analysis of TEM, the large IMC particle was identified as Sn-Cu-Ni ternary compounds, consistenting with the previous EPMA results. Although the stoichiometric fomula of $(Cu,Ni)_6Sn_5$ IMCs was not determined yet, Li et al. reported that a small amount of Ni was incorporated in $(Cu,Ni)_6Sn_5$ IMCs and the diffraction patterns of the $(Cu,Ni)_6Sn_5$ IMCs could be indexed as the standard diffraction pattern of Cu_6Sn_5.[18] In Fig. 8 (a), when the electron diffraction pattern of the ternary Sn-Cu-Ni compounds was exactly matched to the crystal structure of Cu_6Sn_5. For the small IMC particles formed inside the aged SC-0.4Zn solders, Fig.8 (b), they were also identified as the Sn-Cu-Ni-Zn quaternary compounds, consisting of Sn (48.9 at%), Cu (40.1 at%), Ni (3.4 at%) and Zn (7.7 at%). Moreover, the electron diffraction patterns of the quaternary Sn-Cu-Ni-Zn compound were well matched to the crystal structure of Cu_6Sn_5. It implies that the quaternary $(Cu,Ni,Zn)_6Sn_5$ IMCs are also the Cu_6Sn_5. type.

Based on the present experimental findings and thermodynamic calculations, the Cu_6Sn_5

IMCs formed in Sn-0.7Cu can convert to $(Cu,Ni)_6Sn_5$ IMCs by reacting with Ni-P UBMs, and, moreover, they can also change to $(Sn,Ni,Zn)_6Sn_5$ IMCs when Zn was added into Sn-0.7Cu solders. In addition, the Zn atoms incorporated into $(Cu,Ni)_6Sn_5$ IMCs are attributed to suppress coarsening of IMCs particles during thermal aging.

Several studies have reported that Cu_6Sn_5 IMCs were refined by doping Ni atoms in Sn-rich solders.[15,19-20] Kobayashi et al. reported that Cu_6Sn_5 IMCs in the solder matrix were refined by adding 0.05 wt% Ni into Sn-Ag-Cu solders, and the refined $(Cu,Ni)_6Sn_5$ IMCs were effective on increasing the life time of solder joints during bending test.[19] However, Rizvi et al. found that $(Cu,Ni)_6Sn_5$ IMCs coarsened during thermal aging and, moreover, they became larger than Cu_6Sn_5 IMCs after the aging even though they had been finer in the as-reflowed. [20] In the present work, we also observed the coarsening of $(Cu,Ni)_6Sn_5$ during aging in the Sn-0.7Cu solder reacted with Ni-P UBMs, consistent with the previous report.[20] However, the growth of $(Cu,Ni)_6Sn_5$ IMCs during aging was suppressed by the doping of Zn in the solders. This observation is very interesting, and not reported before.

3) Hardness and Shear strength of Sn-0.7Cu-xZn Reacted with Ni-P UBMs

The micro-hardness and ball shear tests were performed to observe the change of mechanical properties associated with the microstructure changes. The Sn-0.7Cu, SC-0.2Zn, SC-0.4Zn and SC-0.8Zn solders reacted with Ni-P during thermal aging were investigated.

Figure 9 shows the hardness results as a function of Zn content as well as aging time. Each sample was reflowed with Ni-P UBMs and aged at 150°C for 500 h. The microhardness of the as-reflowed solders were significantly reduced for Sn-0.7Cu, but not so much for the Zn-added solders. For the as-reflowed Sn-0.7Cu solders, it is quite interesting to note that the

Vickers hardness numbers (VHNs) of Zn-added solders were lowered compared to the Sn-0.7Cu without Zn addition. For the aged solders, Zn addition has gradually increased the microhardness as the Zn content increases

Figure 10(a) shows shear strength of Sn-0.7Cu-xZn solders reacted with Ni-P UBMs. Each sample was reflowed with Ni-P UBMs and aged at 150°C for up to 1000 h. The shear strength of the reflowed Sn-0.7Cu balls reacted with Ni-P UBM was about 330 gF, and then it decreased to less than 300 gF after the aging. In case of Zn-doped solders with Ni-P, the shear strength of the as-reflowed was about 310–320 gF, which was lower than the as-reflowed Sn-0.7Cu solders. However, after aging, the shear strength of the Zn-doped solder joints was higher than the Sn-0.7Cu joints, and, moreover, it was as high as the as-reflowed Zn-doped solders even after aging for 1000 h. Interestingly, the shear strength of the aged in SC-0.8Zn solders with Ni-P UBMs was higher than the as-reflowed. After the shear test, the fracture surface of each sample was examined by SEM and EDS. Figure 10(b) is the SEM images of fracture surfaces of Sn-0.7Cu-xZn with Ni-P UBMs. The EDS composition analysis on the fracture surfaces verified the fracture occurred inside the solder. It means that the shear strength of all solders reacted with Ni-P UBM should be affected by their bulk strength and microstructures.

As discussed earlier, the microstructures of Zn-doped solders with Ni-P UBMs were more stable than Sn-0.7Cu solders during thermal aging. In addition, the large growth of IMC particles in the solder matrix was significantly suppressed by the addition of Zn into Sn-0.7Cu solders. Especially, in case of SC-0.8Zn solders, the microstructures of the aged at 150°C for 500 h were very similar to the as-reflowed. In hardness and shear tests, Zn-doped solders reacted Ni-P UBMs showed more stable mechanical properties during thermal aging, compared to Sn-0.7Cu solders. These stable mechanical properties in Zn-doped solders

during thermal aging are attributed to the incorporation of Zn atoms into (CuNiZn)6Sn5 IMCs and their stable microstructures.

4. Summary

We investigated the effects of minor Zn alloying addition on the interfacial reaction and microstructures of Sn-0.7Cu reacted with electroless Ni-P UBMs during thermal aging at 150°C. In addition, the mechanical properties (hardness and shear strength) of Zn-doped solders were compared with those un-doped solders..

The small amount of Zn added into Sn-0.7Cu solders has modified $(Cu,Ni)_6Sn_5$ IMCs formed at the interface of Ni-P UBMs to $(Cu,Ni,Zn)_6Sn_5$ IMCs. The incorporation of Zn atoms into $(Cu,Ni)_6Sn_5$ IMCs was effective in reducing the IMCs growth during aging, but the effect is not so significant as previously reported with Cu UBM..

The microstructures of Sn-0.7Cu and Zn-doped solders reacted with Ni-P UBMs were much different after thermal aging at 150°C. $(Cu,Ni,Zn)_6Sn_5$ IMC particles were found in the Zn-doped solder matrix, while $(Cu,Ni)_6Sn_5$ IMC particles were observed in the Sn-0.7Cu solders. The incorporation of Zn atoms into $(Cu,Ni)_6Sn_5$ IMCs was very effective on suppressing the growth of IMC particles during thermal aging. $(Cu,Ni,Zn)_6Sn_5$ IMC particles were more stable than $(Cu,Ni)_6Sn_5$ IMC particles during thermal aging at 150°C.

In addition, the stable microstructure of the Zn-doped solders with Ni-P produced stable mechanical properties during thermal aging.

Acknowledgement

We appreciate the support of Dr. Young-Boo Lee and Hyang-Ran Moon at the Korea Basic Science Institute for the EPMA analysis.

References

1. J. Bath, C. Handwerker, and E. Bradley, *Circ. Assemb.* 11, 31 (2000).

2. I.E. Anderson, J.C. Foley, B.A. Cook, J. Harringa, R.K. Terpatra, and O. Unal, *J. Electron. Mater.* 29, 1050 (2001).

3. K.J. Puttlitz, *Handbook of Lead-Free Solder Technology for Microelectronic Assemblies*, ed. K.J. Puttlitz, K.A. Stalter (New York: Marcel Dekker, Inc., 2004), pp. 239–280.

4. S.K. Kang, *Handbook of Lead-Free Solder Technology for Microelectronic Assemblies*, ed. K.J. Puttlitz, K.A. Stalter (New York: Marcel Dekker, Inc., 2004), pp. 281–300.

5. T.C. Chiu, K. Zeng, R. Stierman, D. Edwards, and K. Ano, *Proceedings of the 54th Electronic Components and Technology Conference* (Piscataway, NJ: IEEE, 2004), pp. 1256–1262.

6. M. Date, T. Shoji, M. Fujiyoshi, K. Sato, and K.N. Tu, *Proceedings of the 54th Electronic Components and Technology Conference* (Piscataway, NJ: IEEE, 2004), pp. 668–674.

7. K.S. Kim, S.H. Huh, and K. Suganuma, *Microelectron. Reliab.* 43, 259 (2002).

8. I. de Sousa, D.W. Henderson, L. Patry, S.K. Kang, and D.-Y. Shih, *Proceedings of the 56th Electronic Components and Technology Conference* (Piscataway, NJ: IEEE, 2006), pp. 1454-

1462.

9. S.K. Kang, D.-Y. Shih, D. Leonard, D.W. Henderson, T. Gosselin, S.-I. Cho, J. Yu, and W.K. Choi, *JOM* 56(6), 34 (2004).

10. S.K. Kang, D. Leonard, D.-Y. Shih, L. Gignac, D.W. Henderson, S.-I. Cho, and J. Yu, *J. Electron. Mater.* 35(3), 479 (2006).

11. M.G. Cho, S.K. Kang, D.-Y. Shih, and H.M. Lee, *J. Electron. Mater.* 36(11), 1501 (2007).

12. J.-M.Song, Y.-R. Liu, C.-W. Su, Y.-S. Lai, and Y.-T. Chiu, *J. Mater. Res.* 23(9), 2545 (2008).

13. C.E. Ho, S.C. Yang, and C.R. Kao, *J. Mater. Sci.: Mater. Electron*. 18, 155 (2007).

14. S.-W. Chen and C.-H Wang, *J. Mater. Res.* 21(9), 2270 (2006).

15. F. Gao and T. Takemoto, *J. Alloys Compd.*, 421, 283 (2006).

16. M.G. Cho, S.K. Kang, and H.M. Lee, *J. Mater. Res.* 23(4), 1147 (2008).

17. B. Sundman, B. Jansson, and J.O. Andersson, *CALPHAD 9, 153 (1985).*

18. D. Li, C. Liu, and P.P. Conway, *Mater. Sci. Eng.* A 391, 95 (2005).

19. T. Kobayashi, Y. Kariya, T. Sasaki, M. Tanaka and K. Tatsumi, *Proceedings of the 57th Electronic Components and Technology Conference* (Piscataway, NJ: IEEE, 2007), pp. 684-688.

20. M.J. Rizvi, C. Bailey, Y.C. Chan, M.N. Islam, and H. Lu, *J. Alloys Compd.*, 438, 122 (2007).

Table 1. EDS results of IMC phases formed at the interface between Sn-0.7Cu-xZn solders and Ni-P UBMs after aging at 150°C for 1000 h.

composition (at%)	A	B	C	D
Sn	45.8	46.1	47.7	47.5
Cu	42.7	41.1	34.3	34.2
Ni	11.4	12.5	15.6	12.7
Zn	-	0.32	2.39	5.63

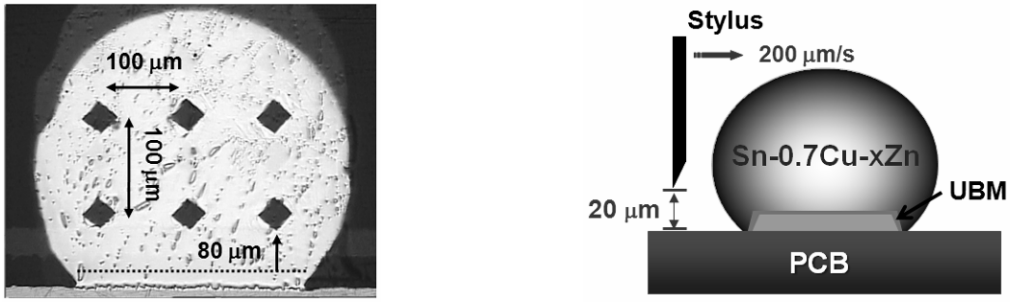

(a) (b)

Figure 1. (a) Typical optical image of the solder joint after hardness test and (b) Schematic image of the ball shear test with a Sn-0.7Cu-xZn solder joint.

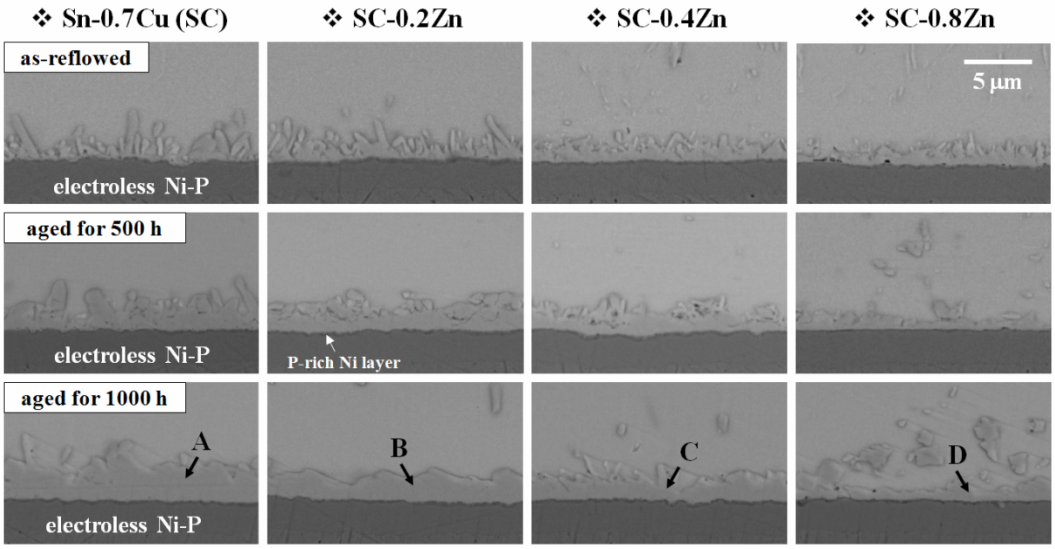

Figure 2. The cross-section images of Sn-0.7Cu-xZn solders on electroless Ni-P UBM after the reflow and aging at 150°C for up to 1000 h.

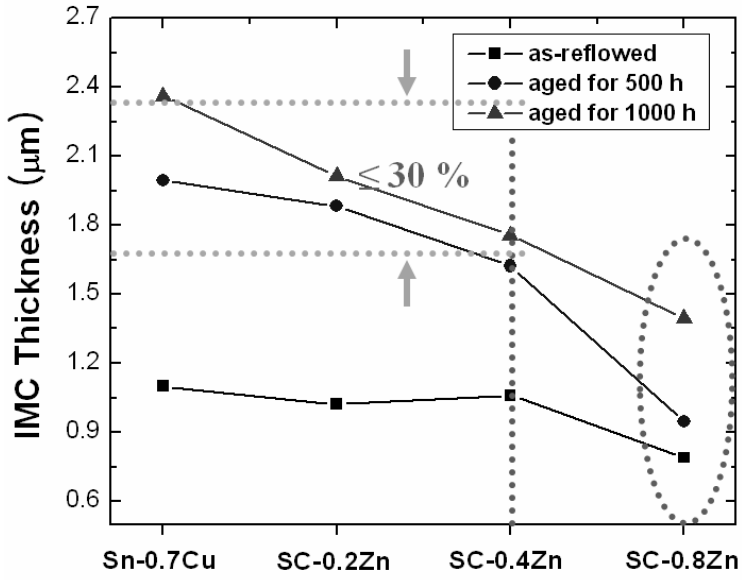

Figure 3. IMCs thickness of each solder after reflow and aging at 150°C for up to 1000 h on electroless Ni-P UBMs.

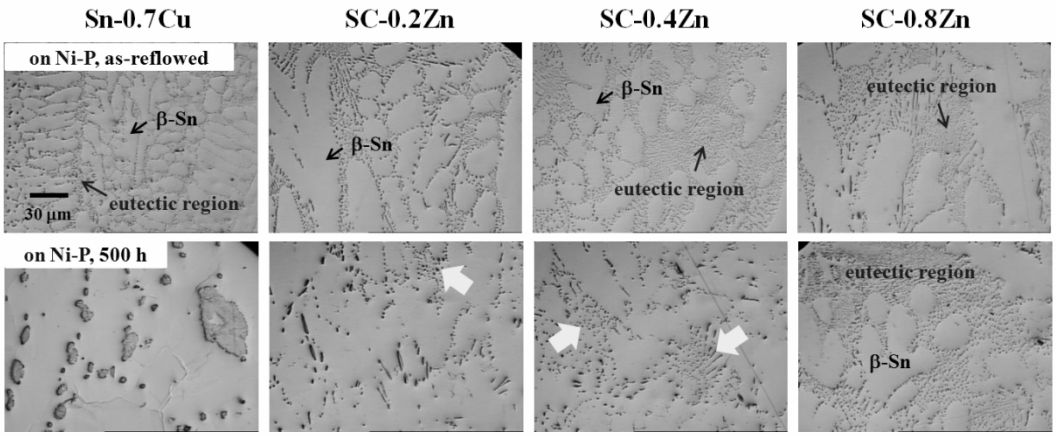

Figure 4. OM images inside Sn-0.7Cu, SC-0.2Zn, SC-0.4Zn and SC-0.8Zn reacted with electroless Ni-P UBMs after reflow and aging at 150˚C for 500 h.

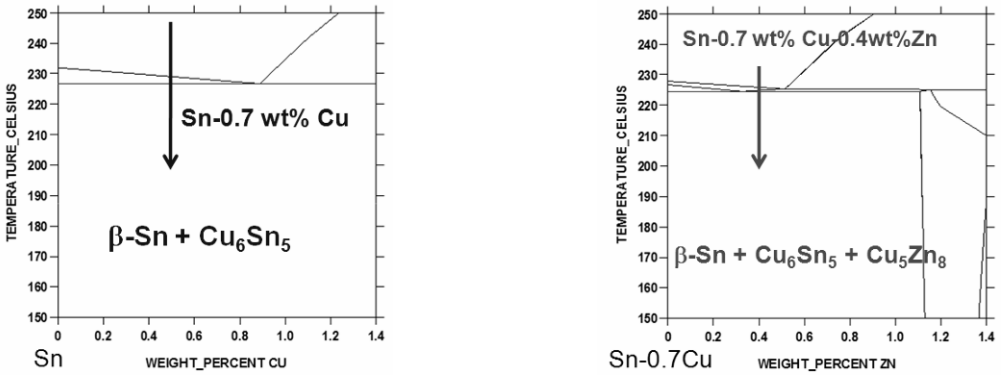

(a) (b)

Figure 5. (a) Equilibrium phase diagram of a Sn-Cu binary system and (b) The vertical section of the Sn-Cu-Zn ternary phase diagram calculated along a constant 99.3:0.7 ratio of Sn/Cu (in wt%).

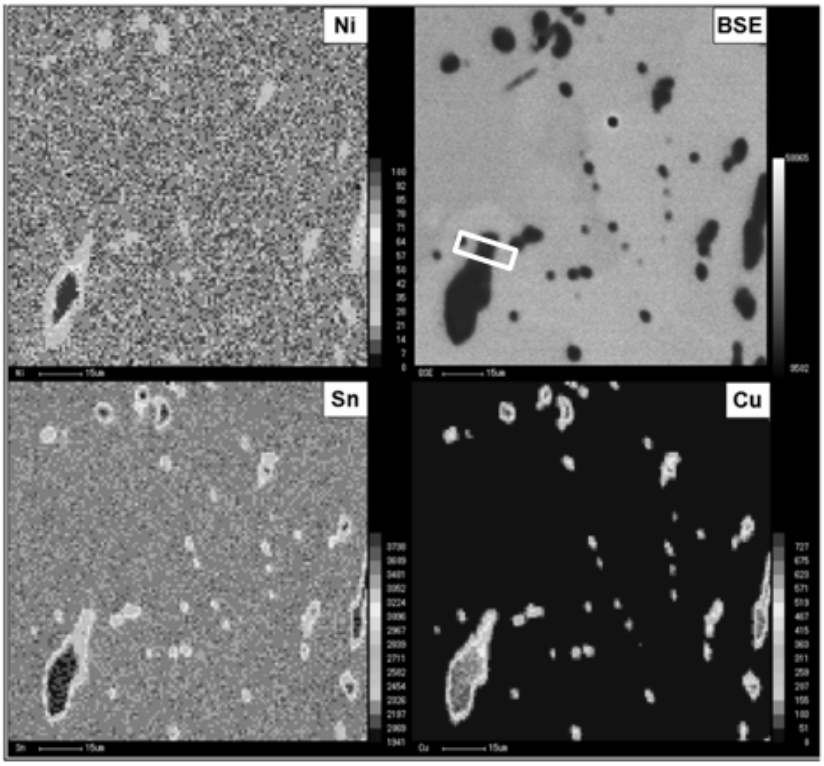

Figure 6. EPMA mapping image of Sn-0.7Cu solder inside that reacted with Ni-P UBMs during aging at 150˚C for 1000 h.

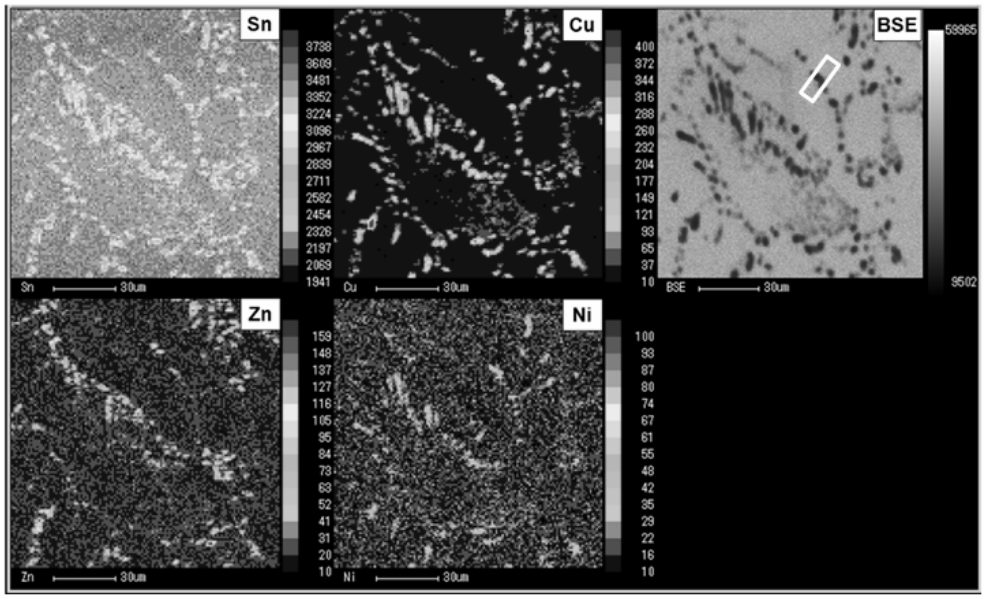

Figure 7. EPMA mapping image of Sn-0.7Cu-0.4Zn solder inside that reacted with Ni-P UBMs during aging at 150˚C for 1000 h.

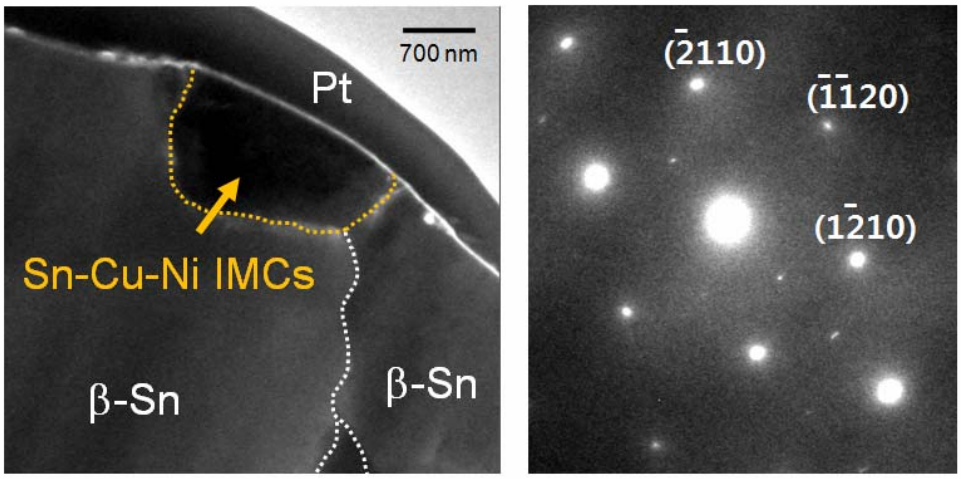

(a)

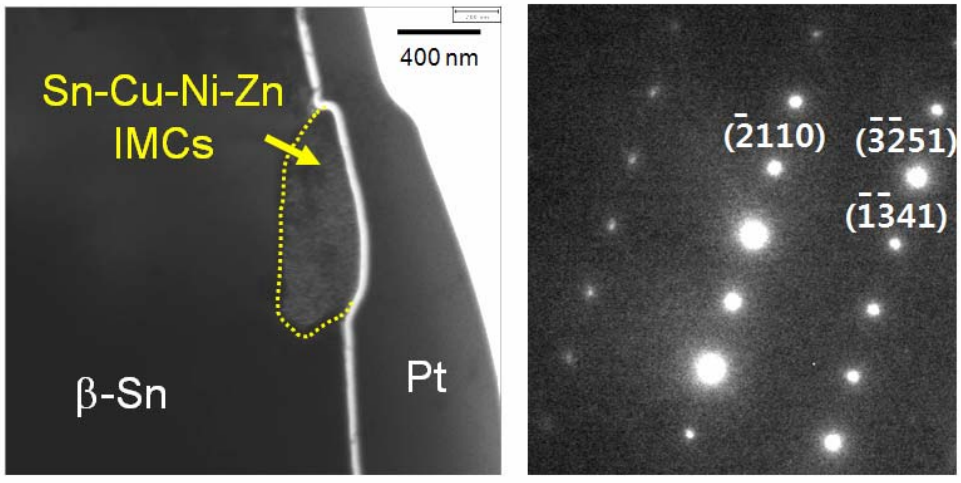

(b)

Figure 8. TEM micrograph and electron diffraction patterns of the IMC particles that formed

inside of (a) Sn-0.7Cu and (a) Sn-0.7Cu-0.4Zn solders after aging at 150˚C for 1000 h.

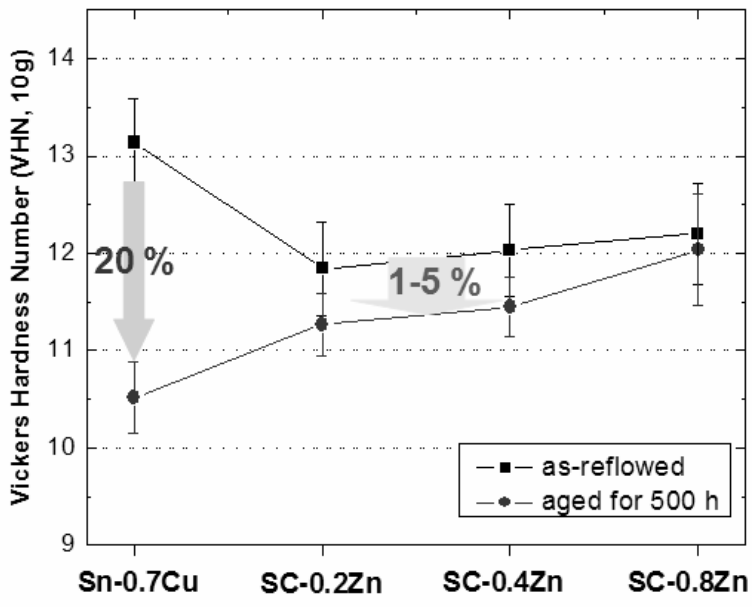

Figure 9. Microhardness results of Sn-0.7Cu-xZn with electroless Ni-P UBMs before and after thermal aging at 150°C for up to 1000 h.

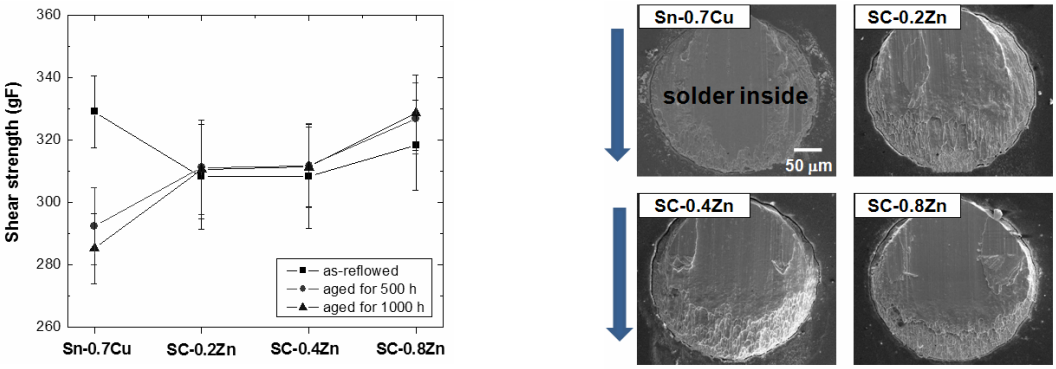

(a) (b)

Figure 10. (a) Shear strength and (b) Fracture surface of Sn-0.7Cu-xZn solders with electroless Ni-P UBMs.